Rate-Adaptive Modulation Techniques for Infrared Wireless Communications

Luciano Diana and Joseph M. Kahn
Department of Electrical Engineering and Computer Sciences
University of California, Berkeley, CA 94720

Abstract

While infrared links can support transmission at high bit rates, it is difficult to maintain a signal-to-noise ratio (SNR) sufficient to support these high bit rates under all conditions using reasonable transmitter power levels. Under adverse conditions, instead of incurring abrupt link failure, it is preferable to achieve graceful degradation by lowering the bit rate until a suitably low error probability can be attained. We describe several coding and decoding schemes for rate-adaptive transmission, and we discuss their performance and implementation complexity. The codes considered are rate-compatible punctured convolutional (RCPC) codes and simple repetition codes. Each code is combined with L-ary pulse-position modulation. We present results of a search for families of good RCPC codes derived from rate-1/5 and rate-1/7 mother codes.

1. Introduction

Indoor wireless communication has gained increasing attention as a viable technology for the implementation of local area networks (LANs). As a transmission medium, infrared (IR) radiation offers several advantages over radio, in particular, a very large unregulated bandwidth and the possibility of reusing the same spectrum in different rooms of a building without interference [1],[2]. User mobility requires that the IR link operate reliably under widely varying channel conditions, which are determined by the ambient light level, the distance between the transmitter and receiver, the degree to which the transmission path is obstructed, the strength of cochannel interference, etc. Link reliability can be enhanced via rate-adaptive transmission. The receiver can estimate the channel conditions and thus the bit rate that can be supported at low error probability. It can convey the recommended bit rate to the transmitter via a feedback channel, so that the transmission rate can be adjusted. A rate-adaptive scheme based on 4-ary pulse-position modulation (4-PPM) with repetition coding [3] is under consideration by the Infrared Data Association (IrDA) for the Advanced Infrared (AIr) standard [4],[5]. In this paper, we describe several alternative rate-adaptive coding schemes. All are based on PPM, which offers good average-power efficiency [6].

The remainder of this paper is organized as follows. In Section 2, we review the modeling of infrared wireless channels. We introduce repetition coding as proposed under AIr in Section 3. In Section 4, we describe a rate-adaptive scheme based on rate-compatible punctured convolutional (RCPC) codes with Viterbi decoding, and we describe a search for families of good RCPC codes derived from rate-$1/5$ and rate-$1/7$ mother codes. In Section 5, we compare the performance of these various schemes. We present concluding remarks in Section 6.

2. Channel Model

Current wireless infrared links use intensity modulation and direct detection (IM/DD), because coherent optical detection is difficult to implement, especially in non-directed links [1],[2]. Let $x(t)$ represent the instantaneous optical power of the transmitter. The constraints on $x(t)$ are

$$x(t) \geq 0 \quad \text{and} \quad \lim_{T \to \infty} \frac{1}{2T} \int_{-T}^{T} x(t)\,dt \leq P_t , \tag{1}$$

where P_t is the average optical power constraint of the transmitter. According to the equivalent baseband model, the received photocurrent is given by:

$$y(t) = r h(t) \otimes x(t) + n(t) , \tag{2}$$

where r is the photodetector responsivity and $h(t)$ is the channel impulse response, which is fixed for a given configuration of transmitter, receiver and intervening reflectors. The average received power is $P_r = H(0) P_t$, where

$$H(0) = \int_{-\infty}^{\infty} h(t)\,dt \tag{3}$$

is the channel d.c. gain. In non-directed links, reflected signals may cause multipath distortion, which can cause intersymbol interference at bit rates above about 10 Mbps [1],[2]. Here, we assume that multipath distortion is negligible, and we model the channel impulse response as $h(t) = H(0)\delta(t)$, where $\delta(t)$ is an impulse function. Wireless infrared links are subject to intense ambient light that gives rise to a high-rate, signal-independent shot noise, which can be modeled as white and Gaussian [1],[2]. We model $n(t)$ as white, Gaussian, and having two-sided power spectral density N_0. Furthermore, $n(t)$ is considered to be independent of the signal $x(t)$.

L-PPM is an orthogonal modulation technique [6] in which a block of $\log_2 L$ input bits is mapped to one of L distinct waveforms, each including one "on" chip and $L - 1$ "off" chips. A rectangular pulse $p(t)$, of duration T_c and amplitude $L \cdot P_t$, is transmitted during the "on" chip. The electrical bandwidth required by a PPM scheme is inversely proportional to T_c; as the bit rate R_b and L are varied, this bandwidth is proportional to $L \cdot R_b / \log_2 L$. The available bandwidth is constrained by the photodetector capacitance and by multipath propagation [1],[2]. It is desirable to mini-

mize the transmitted average optical power P_t in order to minimize power consumption and ocular hazards [1],[2]. In order to evaluate the average power required by various encoding and decoding schemes for a fixed bandwidth requirement, we will compare them in terms of the signal-to-noise ratio (SNR) per chip required to achieve a given probability of error. The SNR per chip is defined as:

$$SNR_{chip} = \frac{r^2 P_r^{\,2}}{N_0} T_c, \tag{4}$$

where r is the detector responsivity. With uncoded L-PPM, $SNR_{chip} = (r^2 P_r^2 / N_0)(1/R_b)(\log_2 L / L)$. The usual SNR per symbol [6] is given by $E_s/N_0 = L^2 \cdot SNR_{chip}$. We note that, since SNR_{chip} is proportional to $P_r^{\,2}$, for a fixed PPM order L, a 1-dB change in the average received optical power yields a 2-dB change in the SNR_{chip}. When L-PPM is combined with an error-correction code of rate $R \le 1$, $SNR_{chip} = (r^2 P_r^2 / N_0)(R/R_b)(\log_2 L / L)$.

3. Repetition Codes

Repetition coding, as proposed under AIr [4], consists of repeating each L-PPM symbol RR times, where RR is the rate-reduction factor. In the AIr scheme, $L = 4$, and RR can take on the values 2, 4, 8, and 16. In the decoding scheme proposed under AIr, the receiver makes chip-by-chip hard decisions, and performs decoding based on a majority-logic scheme. Within a block of RR received symbols, the decoder counts valid symbols (those having a single "on"-chip), and chooses the symbol that makes the largest number of appearances. Several lower and upper bounds for the probability of bit error are given in [7]. In this paper, we use the lower bound:

$$p_b \ge \frac{L}{2(L-1)} \left\{ \left[\binom{n}{t+1} - \eta_{t+1} \right] p^{t+1} (1-p)^{n-t-1} \right\}, \tag{5}$$

where

$$p = Q\left(\sqrt{(L^2/4) \cdot SNR_{chip}}\right) \tag{6}$$

is the channel crossover probability (the probability that a "off"-chip is decoded into a "on"-chip and vice-versa), $t = RR - 1$ is the error-correcting power of the repetition code, $n = RR \cdot L$ is the total number of chips in a block of RR symbols, and η_{t+1} is the number of correctable error patterns of weight $t+1$. Here, $Q(x)$ is the Gaussian Q function [6]. At $p_b = 10^{-9}$, the lower bound (5) is extremely tight for $RR = 1, 2, 4$ and 8, while for $RR = 16$, use of (5) leads to a 0.15-dB underestimate of the optical power requirement.

Improved performance can be obtained using soft-decision decoding (SDD). SDD can be implemented most easily as follows. The block of $RR \cdot L$ chip-rate samples y_k, $k = 0, ..., (RR \cdot L) - 1$ is summed to form a block of L samples z_l, $l = 0, ..., L - 1$, where

$$z_l = \sum_{m=0}^{RR-1} y_{l+mL}, \tag{7}$$

and a conventional soft-decision PPM decoder is used on the z_l. The probability of bit error with SDD is given by:

$$p_b = \frac{L}{2(L-1)} \times$$

$$\left\{ 1 - \frac{1}{\sqrt{2\pi}} \cdot \int_{-\infty}^{\infty} [1 - Q(y)]^{L-1} e^{-\frac{1}{2}\left(y - \sqrt{RR \cdot L^2 \cdot SNR_{chip}}\right)^2} dy \right\}. \tag{8}$$

With SDD, each doubling of RR yields precisely a 3-dB decrease in the value of SNR_{chip} required to achieve a given error probability, corresponding to a 1.5-dB decrease in the required value of the received power P_r. At each value of RR, hard-decision decoding (HDD) requires a value of SNR_{chip} approximately 3 dB higher than SDD.

4. Rate-Compatible Punctured Convolutional Codes

A. Properties

Rate-compatible punctured convolutional (RCPC) codes [8] are a subclass of punctured convolutional codes, which, in turn, are a subclass of the most general convolutional codes. A family of RCPC codes can be obtained from a single *mother code* by periodically deleting some output digits. We restrict our attention to binary RCPC codes, because of the high computational complexity of standard decoding algorithms, in particular the Viterbi algorithm (VA), for high-rate non-binary codes. The parameters that uniquely specify a binary RCPC code are the (N, $K = 1$) binary mother code, of memory M, the puncturing period P, and the $N \times P$ puncturing matrix $\boldsymbol{a}$ [8]. The elements of $\boldsymbol{a}$ are zeros and ones, where the ones indicate the positions of the digits to be transmitted. The period P determines the range of possible rates for all codes derived from the same mother code, which are:

$$R = \frac{P}{P+l} \qquad l = 1, \ldots, (N-1)P. \tag{9}$$

The mother code corresponds to $l = (N-1)P$; it is the lowest-rate code with rate $R_l = 1/N$. The choice $l = 1$ generates the highest-rate code, whose rate is $R_h = P/(P+1)$. Rate compatibility is a restriction on the puncturing matrix [8] that must be imposed when generating different codes within a code family. It states that switching from a lower-rate code to a higher-rate code can only be done by puncturing some digits that has been transmitted in the lower-rate code. Stated differently, switching from a lower-rate code to a higher-rate code must be achieved only by inserting zeros in the puncturing matrix in positions occupied previously by ones, without inserting ones in any positions occupied previously by zeros.

Table 1: Weight spectra of RCPC codes generated with puncturing pattern **a** of period $P = 4$. (a) $(N, K, M) = (5, 1, 2)$ mother code with generators (in octal) of (7, 7, 7, 5, 5).

Pattern **a**	Rate	d_f	$(a_d, d = d_f, d_f + 1,...), [c_d, d = d_f, d_f + 1,...]$
1111 1111 1111 1111 1111	4/20	13	(4, 4, 0, 4, 12 4) [4, 8, 0, 8, 36, 16]
0101 1111 1111 1010 1111	4/16	10	(2, 6, 4, 4, 12, 14) [2, 10, 10, 12, 38, 58]
0000 1111 1111 0000 1111	4/12	8	(8, 0, 20, 0, 52, 0) [12, 0, 60, 0, 232, 0]
0000 0000 1111 0000 1111	4/8	5	(4, 8, 16, 32, 64, 128) [4, 16, 48, 128, 320, 768]
0000 0000 0111 0000 1010	4/5	2	(1, 9, 58, 228, 638, 1597) [1, 21, 387, 1896, 6058, 16767]

(b) $(N, K, M) = (5, 1, 5)$ mother code with generators (in octal) of (75, 71, 73, 65, 57).

Pattern **a**	Rate	d_f	$(a_d, d = d_f, d_f + 1,...), [c_d, d = d_f, d_f + 1,...]$
1111 1111 1111 1111 1111	4/20	22	(4, 12, 4, 4, 4, 4) [8, 28, 8, 12, 16, 12]
0111 1011 1101 1110 1111	4/16	18	(12, 0, 20, 0, 32, 0) [24, 0, 68, 0, 144, 0]
0101 1010 1101 0110 1011	4/12	13	(4, 12, 24, 12, 20, 48) [4, 32, 104, 48, 76, 248]
0001 1000 1100 0110 0011	4/8	8	(4, 28, 28, 32, 68, 92) [8, 116, 128, 128, 328, 460]
0000 1000 0100 0010 0011	4/5	4	(6, 27, 50, 95, 174, 196) [27, 106, 226, 470, 859, 1005]

Such a restriction guarantees that in switching from a higher-rate code to a lower-rate one, the distance of the corresponding transitional path, which is the path in the trellis altered by the code change, is no smaller than the distance of this path within the higher-rate code.

Table 2: Weight spectra of RCPC codes generated with puncturing pattern **a** of period $P = 3$. (a) $(N, K, M) = (7, 1, 2)$ mother code with generators (in octal) of (7, 7, 7, 7, 5, 5, 5).

Pattern **a**	Rate	d_f	$(a_d, d = d_f, d_f + 1,...), [c_d, d = d_f, d_f + 1,...]$
111 111 111 111 111 111 111	3/21	18	(3, 0, 3, 0, 3, 0) [3, 0, 6, 0, 6, 0]
000 111 111 111 000 111 111	3/15	13	(3, 3, 0, 3, 9, 3) [3, 6, 0, 6, 27, 12]
000 000 111 111 000 000 111	3/9	8	(6, 0, 15, 0, 39, 0) [9, 0, 45, 0, 174, 0]
000 000 000 111 000 000 111	3/6	5	(3, 6, 12, 24, 48, 96) [3, 12, 36, 96, 240, 576]
000 000 000 111 000 000 001	3/4	3	(4, 31, 92, 216, 596, 1300) [8, 176, 646, 1788, 5576, 13250]

B. RCPC and *L*-PPM Modulation

In matching binary codes, such as RCPC codes, with non-binary modulation, such as L-PPM, the number of output digits of the code cannot be chosen independent of the order of the modulation scheme. To circumvent this problem we employ the encoding scheme depicted in Fig. 1, which uses a multiplexer followed by $\log_2 L$ identical parallel encoders. We consider two alternative decoding techniques, which are shown in Fig. 1(a) and (b). Fig. 1(a) considers a detector performing soft symbol-by-symbol decisions on L-PPM symbols, followed by a bank of $\log_2 L$ parallel Viterbi decoders, each performing HDD at the bit level. This scheme incurs a performance loss due to HDD, but offers a decoding complexity that depends only weakly on L, since each of the $\log_2 L$ decoders must consider 2^M states, independent of L. As an alternative, we consider using a single Viterbi decoder that performs SDD using chip-by-chip samples, as shown in Fig. 1(b). This solution obtains a performance enhancement from SDD, but the decoding complexity grows rapidly with L, since the single enhanced Viterbi decoder has to consider

Table 2 (cont.): Weight spectra of RCPC codes generated with puncturing pattern **a** of period $P = 3$. (b) $(N, K, M) = (7, 1, 5)$ mother code with generators (in octal) of (53, 75, 65, 75, 47, 67, 57).

Pattern **a**	Rate	d_f	$(a_d, d = d_f, d_f + 1,...), [c_d, d = d_f, d_f + 1,...]$
111 111 111 111 111 111 111	3/21	32	(12, 0, 3, 0, 0, 0) [24, 0, 9, 0, 0, 0]
001 111 110 111 011 011 110	3/15	22	(2, 8, 6, 4, 1, 2) [2, 18, 17, 14, 4, 6]
000 110 110 011 001 001 100	3/9	13	(6, 7, 8, 14, 19, 30) [11, 19, 26, 55, 92, 139]
000 110 000 011 001 001 000	3/6	8	(4, 13, 21, 29, 51, 92) [9, 45, 91, 139, 239, 441]
000 010 000 011 001 000 000	3/4	5	(11, 30, 49, 100, 134, 116) [39, 131, 219, 488, 686, 582]

$2^{M \cdot \log_2 L} = L^M$ states. This complexity is equivalent to that of a non-binary code with $K = \log_2 L$. Currently available Viterbi decoders capable of multi-megabit-per-second operation employ use up to 256 states. As a consequence, if the soft-decoding scheme of Fig. 1(b) is employed, the memory M of a code cannot exceed approximately 4 for 4-PPM and 2 for 16-PPM.

C. Code Search

Families of good RCPC codes derived from rate-$1/2$ mother codes have been tabulated in the literature [8],[9],[10]. These do not provide sufficient variation of coding gain between the lowest- and highest-rate codes for the present application (see (9)). Hence, we have performed a computer search for families of good codes derived from rate-$1/5$ and rate-$1/7$ mother codes. RCPC codes are linear because convolutional codes are linear and because puncturing preserves linearity. L-PPM is not strictly a linear modulation scheme, but can be regarded as linear for purpose of computing error probability, since the Hamming distance between all pairs of codewords is identical. It follows that we can consider the all-zero sequence as the transmitted information sequence, and the corresponding path, corresponding to transmission of a sequence of the zeroth PPM symbol, as the correct path. Important properties of a convolutional code include the free distance d_{free} and the error coefficients a_d and c_d, $d \geq d_{free}$. The coefficient a_d represents the number of error paths at distance d from the all-zero path, while c_d represents the total weight of all these paths, measured in information bits. We have searched for the puncturing patterns that yield codes having the maximum d_{free}. Among puncturing patterns that yield the maximum d_{free}, we have searched for those that yield the minimum value of $c_{d_{free}}$. We note that a cyclic shift of a puncturing pattern yields a code having the same minimum distance and weight spectra [11]. Our search considered rate-1/5 and rate-1/7 mother codes with memory $M \leq 5$ and puncturing period $P \leq 7$. Results for rate-1/5 mother codes with $P = 4$ and with $M = 2$ and $M = 5$ are shown in

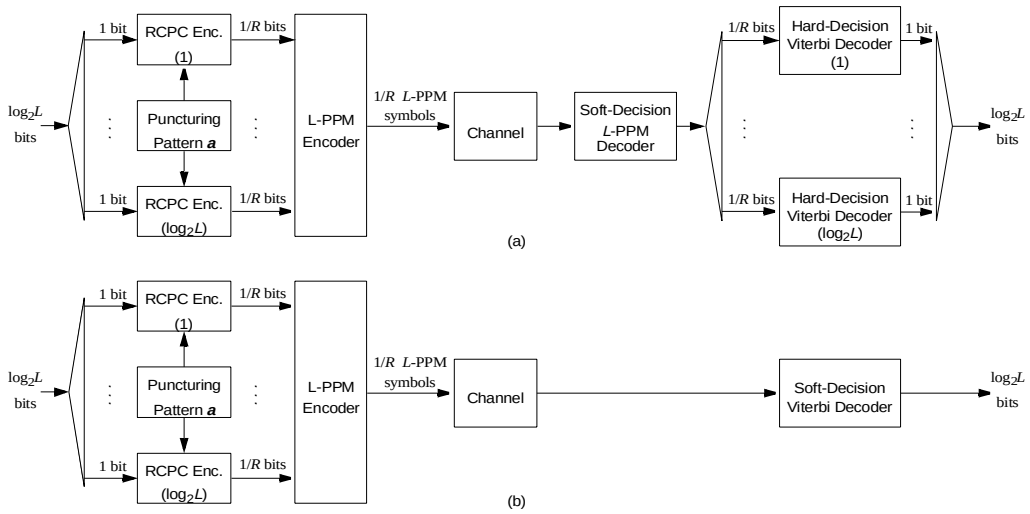

Fig. 1. Methods for encoding and decoding RCPC with L-PPM. Both techniques employ L parallel encoders with a single puncturing pattern ***a***. (a) Symbol-by-symbol soft decisions followed by $\log_2 L$ parallel Viterbi decoders, each performing hard-decision decoding at the bit level. (b) Single enhanced Viterbi decoder performing soft-decision decoding on the chip-rate samples.

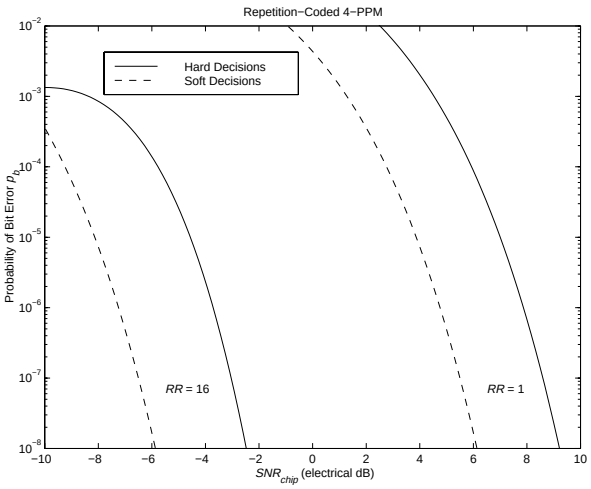

Fig. 2. Comparison between SDD and HDD for repetition-coded 4-PPM. Rate-reduction factors $RR = 1$ and $RR = 16$ are shown. The probability of bit error is evaluated using (5) and (8).

Table 1(a) and (b), respectively. Results for rate-1/7 mother codes with $P = 3$ and with $M = 2$ and $M = 5$ are shown in Table 2(a) and (b), respectively.

Our code search followed the following procedure:

1. Choose an optimal (binary) mother code [6] and a puncturing period *P*. (We choose optimal mother codes under the assumption that optimal mother codes yield good punctured codes [9].) Set all entries of the puncturing matrix **a** to one, corresponding to the lowest-rate (mother) code.
2. Raise the code rate to the next desired rate, thereby determining the number of additional zeros to be inserted in the puncturing matrix **a**. Beginning with the **a** determined at the previous rate, consider all possible patterns for inserting these zeros that are rate-compatible.
3. For each such pattern, search through the trellis to determine d_{free} and the error coefficients a_d and c_d, $d \geq d_{free}$. Discard the code if it is catastrophic. Otherwise, compare d_{free} and $c_{d_{free}}$ with the best values obtained thus far, and store the new code if it is better.
4. Repeat steps 2 and 3 until the highest desired code rate has been reached.

In Table 1 and Table 2, it is evident that the weight coefficients become large as the number of punctured digits increases. This is because error events become long and the multiplicity of the paths at a given distance d from the correct path increases rapidly with increasing d.

An important observation is that if one constructs a code family choosing only a certain set of rates amongst all the possible ones, imposing the rate-compatibility constraint only when necessary leads to the best results. In other words, if going from one code to another implies the puncturing of k digits, searching for the best pattern at each puncturing step will lead after k steps to a code whose performance is worse than the code that would have been found by a direct search.

D. Error-Probability Analysis

With RCPC codes, the VA is performed exactly as with standard convolutional codes, except that the decoder must know the puncturing matrix currently in use and should not update branch metrics at positions occupied by deleted digits. The union bound on the probability of bit error for both HDD and SDD is given by [6]:

$$p_b \leq \frac{1}{P} \sum_{d = d_{free}}^{\infty} c_d P_2(d), \tag{10}$$

where $P_2(d)$ is the probability that an incorrect path at distance d is selected. For the hard-decoding case, $P_2(d)$ is expressed as:

$$P_2(d) = \begin{cases} \displaystyle\sum_{k = (d+1)/2}^{d} \binom{d}{k} p^k (1-p)^{d-k} & d \text{ odd} \\ \displaystyle\sum_{k = d/2+1}^{d} \binom{d}{k} p^k (1-p)^{d-k} + \frac{1}{2}\binom{d}{k} p^{d/2} (1-p)^{d/2} & d \text{ even} \end{cases} \tag{11}$$

Here, p is the channel bit-error probability, which is given by (8) with $RR = 1$. For SDD, the expression for $P_2(d)$ is:

$$P_2(d) = Q(\sqrt{dE_s/N_0}) = Q(\sqrt{dL^2 SNR_{chip}}). \tag{12}$$

5. Performance Evaluation

In this paper, we quantify the SNR efficiency of a coding scheme in terms of the SNR per chip, given by (4), required to achieve a specified bit-error probability p_b, which we take to be 10^{-9}. We quantify the optical power efficiency in terms of the *normalized power requirement*, which is the received average optical power P_r required to achieve the specified value of p_b, normalized to the power required by uncoded on-off keying (OOK) to achieve the same value of p_b. We note that based on the definition of SNR_{chip}, for a fixed PPM order L, a a 2-dB change in the required SNR_{chip} corresponds to a 1-dB change in the normalized optical power requirement. We quantify electrical bandwidth efficiency in terms of the *normalized information rate* R_b/B, where the bandwidth requirement B is defined as the span from d.c. to the first null in the power spectrum of the transmitted waveform.

For OOK, the bit-error probability is computed as

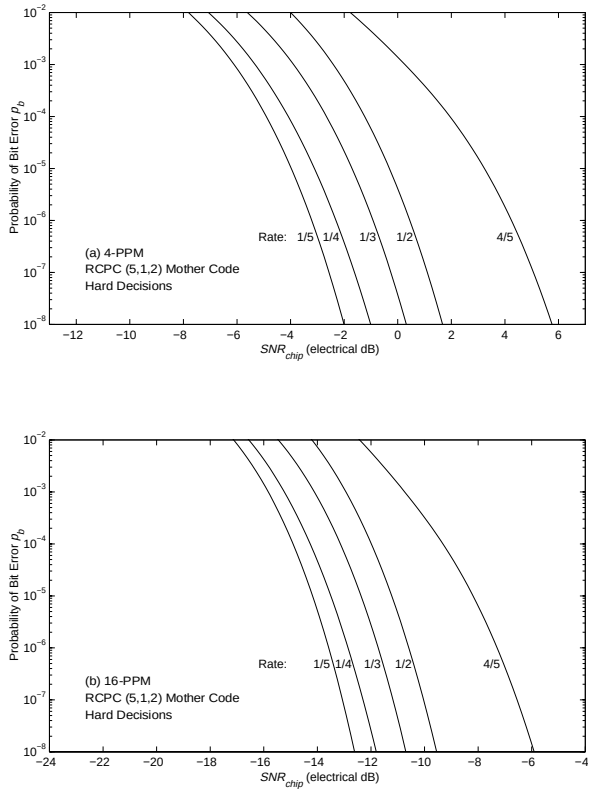

Fig. 3. Bit-error probability for a family of RCPC codes derived from a $(N,K,M) = (5,1,2)$ mother code with puncturing period $P = 4$, as specified in Table 1(a). Hard-decision decoding is performed according to the scheme illustrated in Fig. 1 (a). Only the first two coefficients of the information weight spectra are used to compute these curves, since they give satisfactory accuracy at high SNR. Fractions indicate code rates. (a) 4-PPM. (b) 16-PPM.

$$p_b = Q\left(\sqrt{R^2 P_r^2 / R_b N_0}\right). \tag{13}$$

OOK achieves a normalized optical power requirement of 0 dB and a normalized information rate of unity (assuming the use of rectangular pulses having duration $1/R_b$). For uncoded L-PPM with SDD, the bit-error probability is given by (8) with $RR = 1$. At small p_b, this is well-approximated [2] by the union bound

$$p_b \le (L/2) Q\sqrt{[(L\log_2 L)/2] \cdot (R^2 P_r^2 / R_b N_0)}, \tag{14}$$

which shows that 4-PPM and 16-PPM offer normalized power requirements of −3.0 dB and −7.5 dB, respectively. Uncoded L-PPM achieves a normalized information rate of $R_b/B = \log_2 L / L$, while repetition-coded L-PPM achieves $R_b/B = (1/RR) \cdot (\log_2 L / L)$. For a RCPC of rate R matched with L-PPM modulation, the normalized information rate is $R_b/B = R \cdot (\log_2 L / L)$.

The bit-error probability versus SNR_{chip} for repetition-coded 4-PPM with SDD and HDD is shown in Fig. 2. As previously stated, with SDD, each doubling of the rate-reduction factor RR yields precisely a 3-dB decrease in the value of

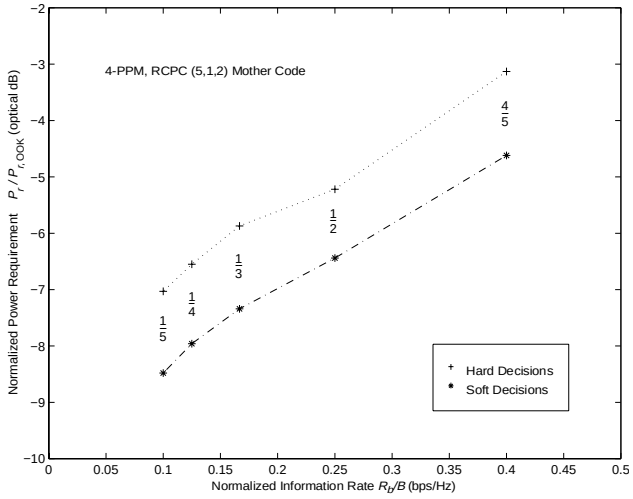

Fig. 4. Comparison of hard- and soft-decision decoding performance of a family of RCPC codes derived from a $(N,K,M) = (5,1,2)$ mother code with puncturing period $P = 4$, as specified in Table 1(a). The fractions indicate code rates. The hard- and soft-decision decoding techniques are depicted in Fig. 1(a) and (b), respectively.

SNR_{chip} required to achieve a given error probability. At each value of RR, HDD requires a value of SNR_{chip} approximately 3 dB higher than SDD, corresponding to a 1.5-dB increase in the normalized power requirement. Thus, with either SDD or HDD, the use of $RR = 16$ provides about a 12-dB reduction in the required SNR_{chip}, compared to the corresponding uncoded case ($RR = 1$). Since SDD is not complex to implement and yields better performance than HDD, only SDD will be considered further here.

Families of RCPC codes provide a variation in the required SNR_{chip} between the strongest and weakest code that is typically less than 10 dB. If one wants to use a high-rate code with rate approaching unity, one has to choose a large value of the puncturing period P. For P exceeding approximately 8 to 10, however, the decision depths of high-rate codes tend to become large, due to the increased number of unmerged paths [12]. Fig. 3(a) and (b) show the bit-error probability versus SNR_{chip} for a family of RCPC codes with 4- and 16-PPM, respectively. This code family is derived from a $(N,K,M) = (5,1,2)$ mother code with puncturing period $P = 4$, as specified in Table 1(a). HDD is performed according to the scheme illustrated in Fig. 1 (a). We see that the variation in required SNR_{chip} between the strongest and weakest code is very similar for 4- and 16-PPM, with 16-PPM requiring a value of SNR_{chip} about 12 dB lower than 4-PPM. With RCPC, the use of HDD increases the required SNR_{chip} by nearly 3 dB compared to SDD, corresponding to nearly a 1.5-dB increase in the normalized power requirement. This is illustrated in Fig. 4 for 4-PPM with the family of codes considered in Fig. 3 (a).

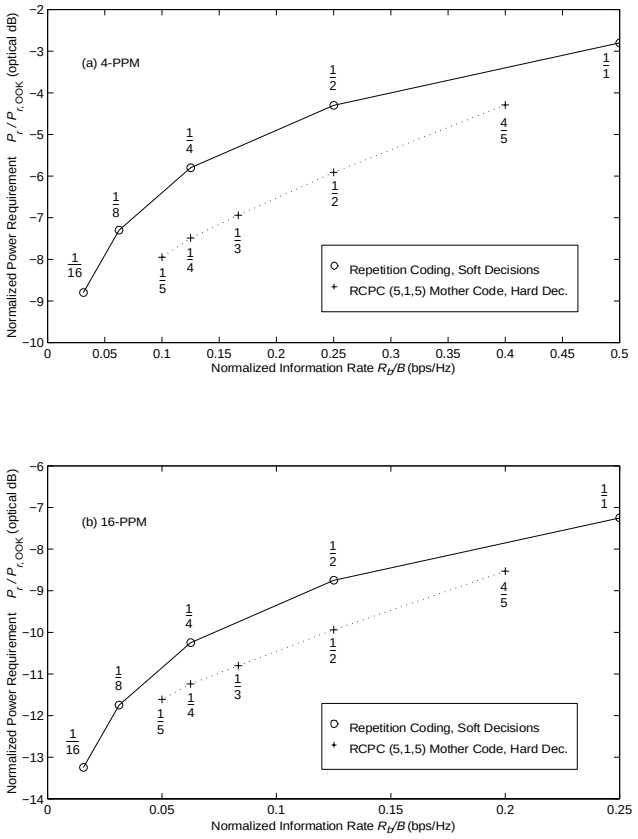

Fig. 5. Normalized power requirements and information rates for repetition codes, and for a family of RCPC codes derived from a $(N,K,M) = (5,1,5)$ mother code with puncturing period $P = 4$, as specified in Table 1(b). Repetition codes utilize soft-decision decoding, while RCPC codes employ the hard-decision decoding technique shown in Fig. 1(a). Both schemes achieve a bit-error probability of 10^{-9}. The fractions indicate code rates.

Fig. 5(a) and (b) compare the normalized power requirements and normalized information rates of two representative coding and decoding schemes with 4- and 16-PPM, respectively. The first scheme utilizes repetition coding with SDD. The second uses a family of RCPC codes derived from a $(N,K,M) = (5,1,5)$ mother code with puncturing period $P = 4$, as specified in Table 1(b), with the HDD technique described in Fig. 1(a). With each particular code, 16-PPM achieves a normalized power requirement of about 4.5 dB lower than 4-PPM, close to the difference in the absence of coding. On the other hand, 4-PPM offers a normalized information rate twice as high as 16-PPM. The repetition-coding scheme yields a 6-dB variation of normalized power requirement in exchange for a 16-fold variation in normalized information rate. It offers very low implementation complexity. The RCPC technique provides 3.1- and 3.7-dB variation of normalized power requirement with 4- and 16-PPM, respectively, both in exchange for a 4-fold variation in normalized information rate. Depending on the information rate, the RCPC scheme offers normalized power requirements as much as 1.7 dB and 1.2 dB less than the repetition-coding scheme, for 4- and 16-PPM, respectively. The decoding complexity of RCPC, while higher than that of repetition coding, is acceptable for many applications.

6. Summary

We have performed a search for families of good RCPC codes derived from rate-$1/5$ and rate-$1/7$ mother codes. We have compared the performance of PPM with repetition codes to that of PPM with RCPC codes, considering both SDD and HDD, on the basis of normalized power requirements and information rates. While repetition codes have somewhat higher normalized power requirements, they offer a wide variation of normalized power requirements and have extremely low implementation complexity, making them attractive for applications in which complexity is highly constrained. The RCPC codes we have considered offer lower normalized power requirements, but achieve a smaller variation of normalized power requirements and have higher decoding complexity.

7. Acknowledgments

This research was supported by National Science Foundation Grant Number ECS-9710065, LG Electronics, Hewlett-Packard, and the University of California MICRO Program.

8. References

1. J.M. Kahn and J.R. Barry, "Wireless Infrared Communications", *Proc. of the IEEE*, vol. 85, no. 2, pp. 265-98, Feb. 1997.
2. J.R. Barry, *Wireless Infrared Communications*, Boston, Kluwer Academic, 1994.
3. M. De Lange, F. Gfeller, W. Hirt and B. Weiss. "Wireless Infrared Transmission: How To Reach All Office Space", *Proc. of IEEE Vehicular Technol. Conf.*, pp. 1535-1539, April 1996, Atlanta, Georgia.
4. Infrared Data Association, *Request for Comments of Advanced Infrared IrMAC Draft Protocol Specification*, April 8, 1997.
5. Infrared Data Association, *Serial Infrared (SIR) Physical Layer Link Specification*, April, 1994.
6. J.G. Proakis, *Digital Communications*, 3rd Edition, McGraw-Hill, 1995.
7. F. Chow and J.M. Kahn, "Effect of Non-Reciprocity on Infrared Wireless Local-Area Networks", subm. to *IEEE Trans. on Commun.*, March, 1999. Available at: `http://www.eecs.berkeley.edu/~jmk/res.areas/irwc.html`.
8. J. Hagenauer, "Rate-Compatible Punctured Convolutional Codes (RCPC) Codes: Structure, Properties and Construction Techniques", *IEEE Trans. on Commun.*, vol. 36, no. 4, pp. 389-400, 1988.
9. L.H.C. Lee, "New Rate-Compatible Punctured Convolutional Codes for Viterbi Decoding", *IEEE Trans. on Commun.*, vol. 42, no. 12. pp. 3073-3079, 1994.
10. J. Geist, J. Cain and G. Clark, "Punctured Convolutional Codes of Rate $(n-1)/n$ and Simplified Maximum Likelihood Decoding." *IEEE Trans. on Information Theory*, vol. IT-25, pp. 97-100, 1979.
11. I.G. Begin and D. Haccoun, "High-rate Punctured Convolutional Codes: Structure, Properties and Construction Technique", *IEEE Trans. on Commun.*, vol. 37, no.12, pp. 1381-1385, Dec. 1989.
12. G.C.Clark and Jr., J.B.Cain, *Error-Correction Coding for Digital Communications*, Plenum Press, New York, 1981.